American Journal of Climate Change, 2023, 12, 292-320
https://www.scirp.org/journal/ajcc
ISSN Online: 2167-9509
ISSN Print: 2167-9495

Analysis of Weather Anomalies to Assess the 2021 Flood Events in Yaounde, Cameroon (Central Africa)

Tatiana Denise Nimpa Fozong[1,2*], Ojuku Tiafack[1], Simeon Tchakonte[3], Christiane Guillaine Nimpa Ngeumo[4], Dominique Badariotti[2]

[1]Department of Geography, University of Yaounde 1, Yaounde, Cameroon
[2]Image, City and Environment Laboratory, Faculty of Geography and Planning, University of Strasbourg, Strasbourg, France
[3]Department of Environmental Science, Faculty of Science, University of Buea, Buea, Cameroon
[4]Department of Geography and Planning, Faculty of Arts, University of Bamenda, Bambili, Cameroon
Email: *nimpatatiana580@gmail.com

How to cite this paper: Fozong, T. D. N., Tiafack, O., Tchakonte, S., Ngeumo, C. G. N., & Badariotti, D. (2023). Analysis of Weather Anomalies to Assess the 2021 Flood Events in Yaounde, Cameroon (Central Africa). *American Journal of Climate Change, 12,* 292-320.
https://doi.org/10.4236/ajcc.2023.122014

Received: April 7, 2023
Accepted: June 27, 2023
Published: June 30, 2023

Copyright © 2023 by author(s) and Scientific Research Publishing Inc.
This work is licensed under the Creative Commons Attribution International License (CC BY 4.0).
http://creativecommons.org/licenses/by/4.0/
Open Access

Abstract

Extreme weather anomalies such as rainfall and its subsequent flood events are governed by complex weather systems and interactions between them. It is important to understand the drivers of such events as it helps prepare for and mitigate or respond to the related impacts. In line with the above statements, quarter-hourly data for the year 2021 recorded in the Yaounde meteorological station were synthesized to come out with daily and dekadal (10-day averaged) anomalies of six climate factors (rainfall, temperature, insolation, relative humidity, dew point and wind speed), in order to assess the occurrences and severity of floods to changing weather patterns in Yaounde. In addition, Precipitation Concentration Index (PCI) was computed to evaluate the distribution and analyse the frequency and intensity of precipitation. Coefficient of variation (CV) was used to estimate the seasonal and annual variation of rainfall patterns, while Mann-Kendall (MK) trend test was performed to detect weather anomalies (12-month period variation) in quarter-hourly rainfall data from January 1st to December 31st 2021. The Standard Precipitation Index (SPI) was also used to quantify the rainfall deficiency of the observed time scale. Results reveal that based on the historical data from 1979 to 2018 in the bimodal rainfall forest zone, maximum and minimum temperature averages recorded in Yaounde in 2021 were mostly above historical average values. Precipitations were rare during dry seasons, with range value of 0 - 13.6 mm for the great dry season and 0 - 21.4 mm for the small dry season. Whereas during small and great rainy seasons, rainfalls were regular with intensity varying between 0 and 50 mm, and between 0 and 90.4 mm,

respectively. The MK trend test showed that there was a statistical significant increase in rainfall trend for the month of August at a 5% level of significance, while a significant decreasing trend was observed in July and December. There was a strong irregular rainfall distribution during the months of February, July and December 2021, with a weather being mildly wetted during all the dry seasons and extremely wetted in August. Recorded flooding days within the year of study matched with heavy rainy days including during dry seasons.

Keywords

Weather Variability Analysis, Rainfall Anomalies, Precipitation Indices, Flood Hazard, Yaounde-Cameroon

1. Introduction

Weather factors are expected to intensify with global warming, which likely increases the intensity of extreme precipitation events and the risk of flooding (Tabari, 2020). The 6th report of the Intergovernmental Panel on Climate Change (IPCC, 2023) stated that Teleconnections to major climate modes, such as the El Niño-Southern Oscillation (ENSO) or the Indian Ocean Dipole (IOD), strongly influence seasonal rainfall anomalies and rainy season timing in large parts of Africa, in turn affecting the inter-annual variability in river flows. According to the World Meteorological Organisation (WMO, 2022), a third of deaths due to extreme weather events linked to climate variability over the past 50 years have occurred in Africa. Tramblay et al. (2021) reported that Africa is severely affected by floods, with an increasing vulnerability to these events in the most recent decades.

From the Far North region of Cameroon (with a particularly hot and dry Sudano-Sahelian climate type and a mono-modal rainfall), to the Centre-Southern forest region (with a wet tropical and equatorial climate type and a bimodal rainfall), passing through the Littoral and great West regions (with a wet tropical and equatorial climate type and a mono-modal rainfall), floods have occurred every year, both during dry and rainy seasons, and this has been the case for the past several decades (Zogning et al., 2016; Djiangoué, 2017; Zogning, 2017; Saha & Tchindjang, 2017; Tanessong et al., 2017; Mboka et al., 2020; Nsangou et al., 2022; Onana et al., 2022). The cities of Maroua (in the Far North region), Douala (in the Littoral region) and Yaounde (in the Centre region) are the most flood prone cities of the country with frequent flood events in recent years and significant damage to livestock, infrastructure, economy and loss of life (MINEPDED, 2015). In 2021, Yaounde was once again hit by severe floods, with the worst affected areas being in the central and southern parts of the city. Streets and buildings were flooded and vehicles stranded. Very few studies have so far been carried out to assess flood phenomenon in Yaounde. Most of these previous

works deal with geomorphology, uncontrolled urbanisation and poor settlement in lowlands (Assako Assako, 1997; Mediebou, 2023), the hydrological characteristics (discharge) of the watershed/basin (Ebode, 2022) as risk drivers of flooding in Yaounde. Other investigations deal with agricultural development, land use practices, pollution and emergent of waterborne diseases related to flood risk areas (Tchekote et al., 2019). Very few studies focused on the contribution of geographic information systems (GIS) for the mapping of flooding factors in Yaounde (Zogning et al., 2016; Zogning, 2017); while others looked at urban flood susceptibility modelling in the Mfoundi watershed using Analytical Hierarchy Process (AHP) and GIS (Nsangou et al., 2022; Onana et al., 2022).

Flood hazard assessment in Yaounde has been rarely, if ever, addressed along with the global climate factors and indices; available data are scarce, fragmentary or partial (not including all the 7 subdivisions of Yaounde, or not covering the entire Mfoundi watershed from upstream to downstream). To the best of our knowledge, no study has so far combined on-site recorded quarter-hourly climate data and computation of precipitation indices and statistical tests to assess flood hazard in Yaounde. It is well documented that climate events can be measured by tracking their frequency to assess their impacts on floods. Understanding the underlying climate causes of these flood events and their trends over time is crucial for effective disaster management and planning, and designing of mitigation measures in the context of climate change. The purpose of this study was to analyse weather anomalies in relation with the 2021 flood events in Yaounde. To achieve this objective, the quarter-hourly daily data of major weather metrics including rainfall, temperature, insolation, relative humidity, dew point and wind speed recorded during the year 2021 were analysed and their relationships with rainy and flooded days were determined. In addition, precipitation indices and statistical tests were performed to assess rainfall distribution, and intensity. Furthermore, the dekadal weather alerts and forecasts made by the Cameroon National Observatory on Climate Change for the study period based on historical data (1979-2018) were examined and gaps identified.

2. Materials and Methods

2.1. Study Area

This study was carried out in the city of Yaounde, the political capital of Cameroon which has a population estimated at 3.32 million (NIS, 2019). It is found in the Centre Region of the nation, between latitude 3˚30' & 3˚58' North and longitude 11˚20' & 11˚40' East, with an average elevation of about 750 m (**Map 1**). The climate of Yaounde was redefined and classified by Sighomnou (2004) as a transitional wet tropical and equatorial type with four unevenly distributed seasons: a great rainy season (from August to November), a great dry season (from December to February), a small rainy season (from March to June) and a small dry season (July). Total precipitation here is around 1600 mm per year. The rainy seasons are of unequal lengths and are characterised by heavy rains

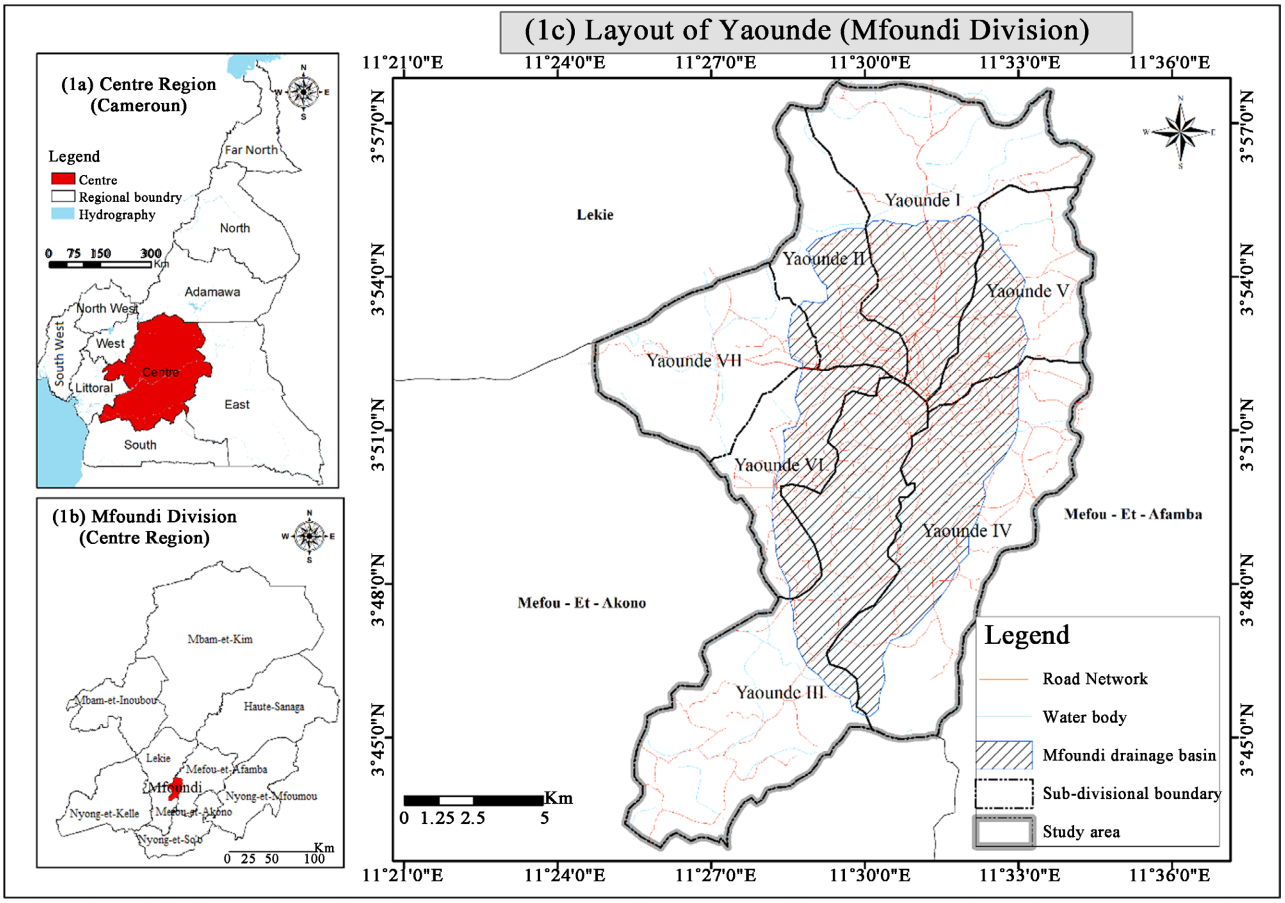

Map 1. Location map of the study area.

often concentrated in time. Yaounde belongs to the half-deciduous forestry zone deeply affected by man. Yaounde Highlands are a compartment of mountains that form a defensive wall along the western part of the city. These hills and mountains alter the patterns of wind circulation, rainfall and temperature.

2.2. Data

The data applied include recorded flooding event days in Yaounde within the year 2021 with affected neighbourhoods. Quarter-hourly weather data of six climate parameters including rainfall, temperature, insolation, relative humidity, dew point and wind speed were obtained from the Agro-ecological meteorological station of Yaounde. Dekadal bulletins on weather forecasts and alerts based on historical data (1979-2018) and data from the Climate Research Unit, done by the National Observatory on Climate Change (NOCC) for the study period were consulted and climate data of temperature and rainfall were obtained, analysed and compared with the current trends.

2.3. Data Analysis Techniques

Numerous tests are available to study the long-term change of climate parameters over time. Measuring the changes of observed climate trends and variability

over time was done using different techniques which included Precipitation Concentration Index (PCI) to evaluate the distribution and analyse the frequency and intensity of the precipitation. Coefficient of variation (CV) was used to estimate the seasonal and annual variation of the rainfall patterns and Mann-Kendall (MK) trend test to detect climate trend in times series data. Additionally, the Standard Precipitation Index (SPI) was used to quantify the rainfall deficiency of the observed time scale in the given watershed (Svoboda et al., 2012; Hänsel et al., 2016; Asfaw et al., 2018; Esayas et al., 2019).

2.3.1. Coefficient of Variation (CV)

Coefficient of Variation (CV) is a dimensionless metric of variability used to statistically measure how the individual data points vary about the mean value. In this study, CV was computed on daily time series data derived from the quarter-hourly data, to detect monthly and annual rainfall variability for the year 2021. As documented by Hare (2003), the degree of rainfall variability is classified as high (CV > 30), moderate (20 < CV > 30) and low (CV < 20). Hence the higher the value of CV the higher the variability of rainfall in the study region and the reverse is also true. The values of CV were computed using Equation (1):

$$\mathrm{CV} = \frac{\sigma}{\mu} \times 100$$

where CV is the coefficient of variation, σ is the standard deviation and μ is the mean precipitation of the recording period.

2.3.2. Precipitation Concentration Index (PCI)

Precipitation Concentration Index (PCI) was used to evaluate the monthly and annual distribution of rainfall. PCI is used to indicate the hydrological risks of floods and drought occasions in the study area (De Luis et al., 2000; Gocic & Trajkovic, 2013) and can be calculated using Equation (2):

$$PCI = \frac{\sum_{i=1}^{12} pi^2}{\left(\sum_{i=1}^{12} pi\right)^2} 100$$

where *Pi* is monthly precipitation in the month i. The values of PCI along with their interpretations are given in Table 1. In this study, PCI was computed for monthly period with daily time series data derived from the quarter-hourly data recorded throughout the year 2021. Furthermore, statistics employed in the

Table 1. Precipitation Concentration Index (PCI) and its interpretation (Oliver, 1980).

PCI value	Interpretation
≤10	Uniform rainfall distribution
[10 - 15]	Moderate rainfall distribution
[15 - 20]	Irregular rainfall distribution
>20	Strong irregular rainfall distribution

analysis include Pearson Product Moment Correlation (PPMC) to establish the relationship between PCI and annual rainfall and further between PCI and number of rainy days. The calculation was performed using the Statistical Package for Social Sciences (SPSS) version 20.

2.3.3. Standard Precipitation Index (SPI)

Standard Precipitation Index (SPI) is a probability (i.e. statistical) index used to study relative departures of precipitation from normality, which gives a representation of abnormal wetness and dryness. The SPI is the most widely used method of drought index to detect and characterize meteorological drought (Karabulut, 2015). SPI can be calculated for different periods (1, 3, 6, 12, 24, and 48 months) (Svoboda et al., 2012). In this study, SPI was computed for monthly period with daily time series data derived from the quarter-hourly data recorded throughout the year 2021. SPI value was calculated by using Equation (3):

$$SPI_{ij} = \frac{X_{ij} - \mu_{ij}}{\alpha_{ij}}$$

where the SPI_{ij} represents an i^{th} month at j^{th} period, X_{ij} is the observed rainfall total value for the i^{th} month at the j^{th} period; μ_{ij} and α_{ij} represents the long-term mean and standard deviation of the i^{th} month and j^{th} timescale of the selected period respectively. According to the study conducted by Svoboda et al. (2012), SPI has different output values ranging from ≤−2.0 to ≥2.0 (**Table 2**)

2.3.4. Mann-Kendall (MK) Trend Test and Sen's Slope Estimator Test

The Mann-Kendall (MK) trend test is one of the widely used methods to detect climate trend in time series data. The details of the MK test are provided in (Mann, 1945). The MK test is used to detect monotonically (increasing or decreasing) trends of annual and seasonal bases of climate parameters. To investigate the existence of long-term change for both rainfall and temperature indices, Mann-Kendall (MK) trend test and Sen's slope estimator test were employed. Annual and seasonal trend change detection with the MK test is less affected by climate outliers (Sen, 1968; Birsan et al., 2005). However, the result of the MK

Table 2. Standard Precipitation Index (SPI) range and its interpretation.

SPI value	Interpretation
2.0 or more	Extremely wet
1.5 to 1.99	Severely wet
1.0 to 1.49	Moderately wet
0.99 to 0	Mildly wet
0 to −0.99	Mild drought
−1.0 to −1.49	Moderately dry
−1.5 to −1.99	Severely dry
−2.0 or less	Extremely dry

test may contain some errors if autocorrelation exists in the time series data. To overcome this problem, the pre-whitening procedure was performed and there was no significant level of serial autocorrelation at all lags and performed without any modification. Following the serial autocorrelation test, the MK test from the Z value and trend from Sen's slope (β) estimation were computed based on daily period data derived from the quarter-hourly rainfall data recorded throughout the year 2021 (January 1st - December 31st).

The Mann-Kendall Test is used to determine whether a time series has a monotonic upward or downward trend, with a confidence level of 95%. It does not require that the data be normally distributed or linear. It does require that there is no autocorrelation. The null hypothesis (H_0) for this test is that there is no trend, and the alternative hypothesis (H_a) is that there is a trend in the two-sided test or that there is an upward trend (or downward trend) in the one-sided test. Note that if MK > 0 then later observations in the time series tend to be larger than those that appear earlier in the time series, while the reverse is true if MK < 0. These tests were performed using XL-STAT 2014.

3. Results

3.1. Trends of Weather Metrics and Precipitation Indices

The climate of Yaounde is a transitional wet tropical and equatorial type with four unevenly distributed seasons (Sighomnou, 2004; Nguemou, 2008): a small rainy season from March to June with total rainfall of 689 mm and an average temperature of 24.18˚C; a small dry season (July) with total rainfall of 38.4 mm and an average temperature of 22.81˚C; a great rainy season (August to November) with total rainfall of 1225 mm and an average temperature of 23.21˚C; and a great dry season (December to February) with total rainfall of 58.6 mm and an average temperature of 25.19˚C (**Figure 1**). The total rainfall and average temperature in Yaounde for the year 2021 (January 1st - December 31st 2021) are 2011 mm and 24˚C ± 1˚C, respectively.

3.1.1. Analysis of Precipitation Trends and Indices

Figure 2 depicts the daily rainfall variation in the Yaounde urban area for the period from January 1st to December 31st 2021. Results reveal that precipitations were rare and scarce during dry seasons (but not absent), with range value of 0 - 13.6 mm for the great dry season and 0 - 21.4 mm for the small dry season. Whereas during the small (March to June) and great (August to November) rainy seasons rainfalls were regular with intensity varying between 0 and 50 mm, and between 0 and 90.4 mm, respectively. Rainfall was more regular in May and October whereas the rainfall intensity was high in June, August, September and October.

Figure 3 presents the dekadal and monthly numbers of rainy days in the Yaounde urban area for the period from January 1st to December 31st 2021. Results show that a total of 161 rainy days were recorded all over the year. During dry seasons rainfall was rare and scarce with 4 rainy days recorded only during

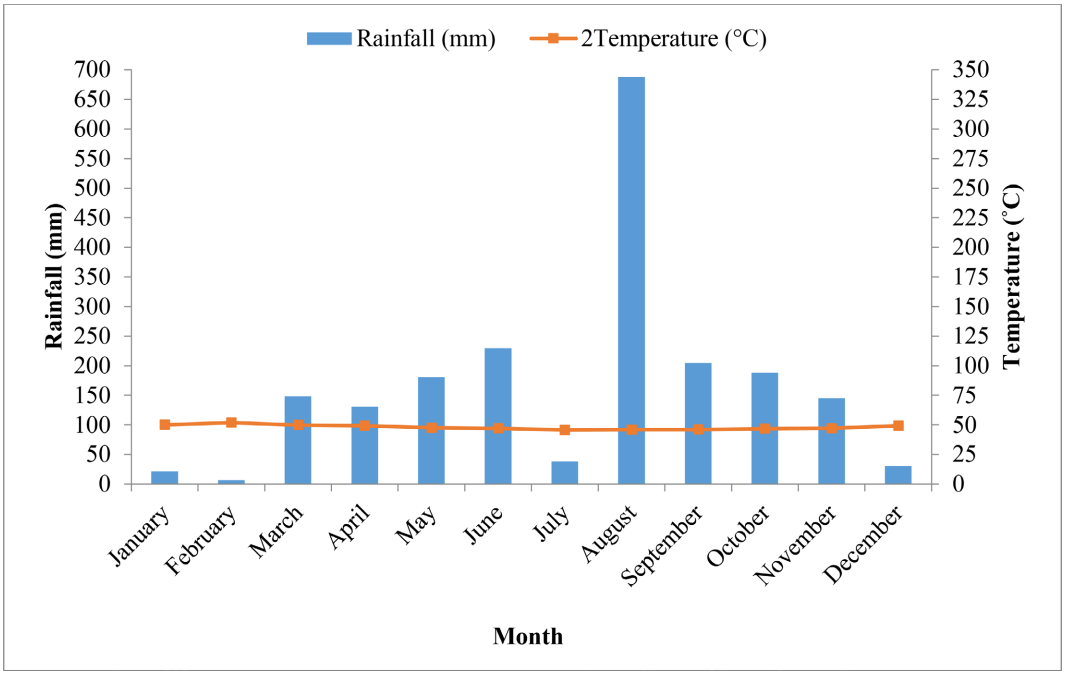

Figure 1. Ombrothermal diagram of the Yaounde city, based on the mean hourly variations of rainfall and air temperatures for the year 2021.

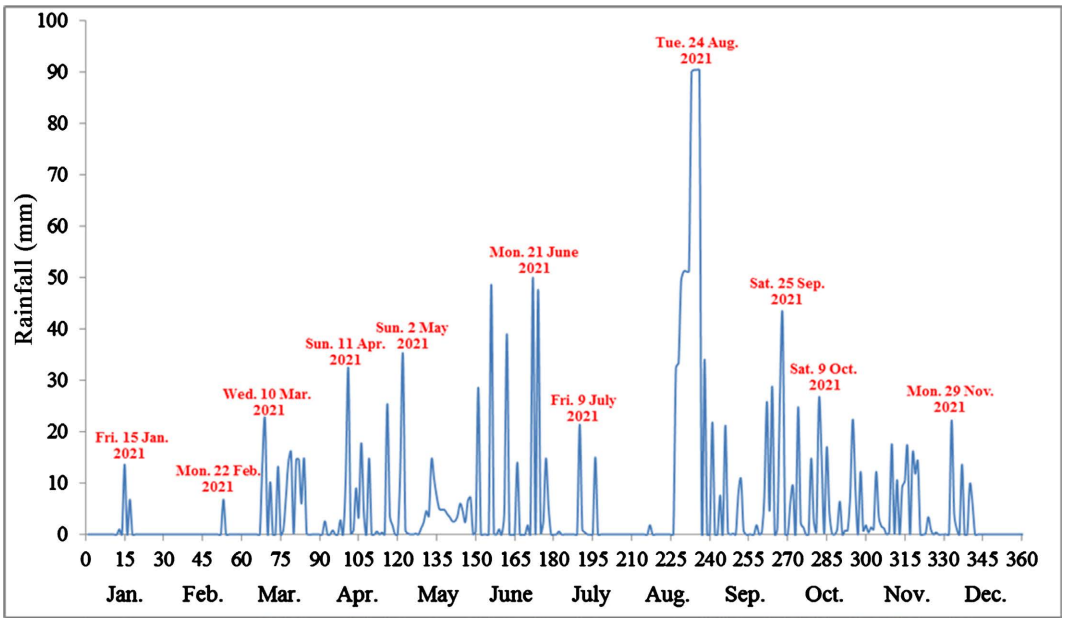

Figure 2. Daily rainfall variation in Yaounde urban area during the year 2021; information in red shows the day of the month with the highest rainfall intensity.

the first dekad of December (1 3, 6 and 7 December), and 3 in January, all during the second dekad (13, 15 and 17 January); whereas it rained just once in February (22 February), and during 5 days in July (1, 9, 10, 11 and 15 July). During the small rainy season, rainfalls were regular with a total number of 71 rainy days distributed as follow: 14, 17, 27 and 13 days recorded during the months of March, April, May and June, respectively. Likewise, all over the great

rainy season, rainfalls were regular with a total number of 77 rainy days distributed as follow: 14, 18, 26 and 19 days recorded during the months of August, September, October and November, respectively.

Figure 4 depicts the monthly variation of the Standard Precipitation Index (SPI) computed with daily rainfall data of the Yaounde urban area for the period from January 1st to December 31st 2021. It results from the analysis that throughout the year 2021, the weather was mildly wetted during all the months of dry seasons (December, January, February, and July) and some months of

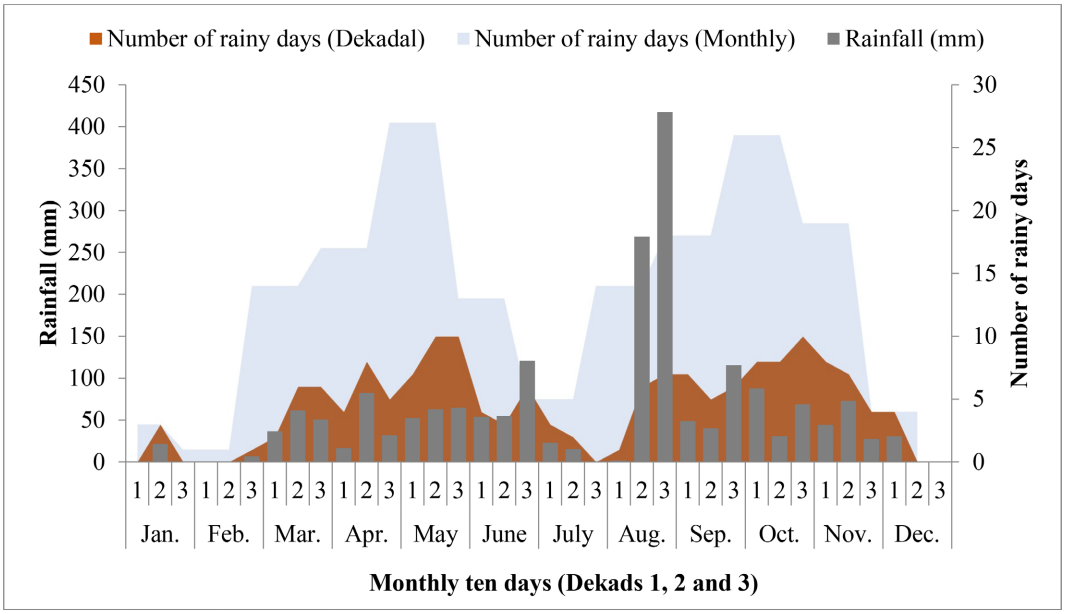

Figure 3. Average dekadal and monthly number of rainy days, and rainfall in Yaounde during the year 2021.

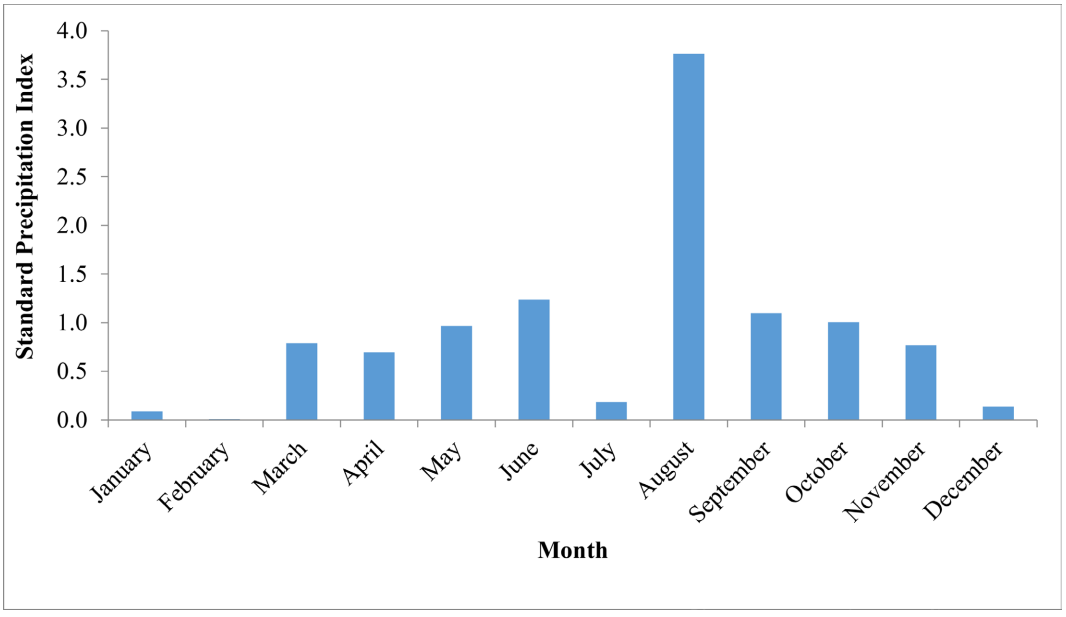

Figure 4. Monthly variation of Standard Precipitation Index computed with daily rainfall data for the year 2021.

rainy seasons (March, April, May and November), whereas the weather was moderately wetted in June, September and October, and extremely wetted in August.

Figure 5 shows the monthly variation of the Precipitation Concentration Index (PCI) computed with daily rainfall data of the Yaounde urban area for the period from January 1st to December 31st 2021. It results from the analysis that throughout the year 2021, rainfalls were uniformly distributed in March (PCI = 9.86), May (PCI = 8.99), August (PCI = 9.87), October (PCI = 8.72) and November (PCI = 9.77). Moderate rainfall distribution was observed during the months of April (PCI = 14.46) and September (PCI = 11.82), whereas irregular rainfall distribution was noticed in June (PCI = 17.33). During all the months of dry seasons (December, January, February, and July) a strong irregular rainfall distribution was registered, with PCI values widely above 20.

The computed summary statistics of monthly precipitation (derived from quarter-hourly daily precipitation) including minimum (Min.), maximum (Max.), total, standard deviation (SD), rainfall distribution, and coefficient of variation (CV) in Yaounde urban area for the period from January 1st to December 31st 2021 are presented in Table 3. The total annual rainfall was recorded as 2011 mm with a standard deviation of 181.29 mm. The three months with the highest total monthly rainfall are August (688 mm), June (229.4 mm) and September (201.4 mm) which contributed 34.21%, 11.41% and 10.16% to the total rainfall respectively. December, January and February received the least rainfall (30.4, 21.4 and 6.8 mm respectively) and contributed 1.51%, 1.06% and 0.34% to the annual rainfall respectively.

The CV of the inter-monthly total rainfall revealed a high (108.18%) rainfall

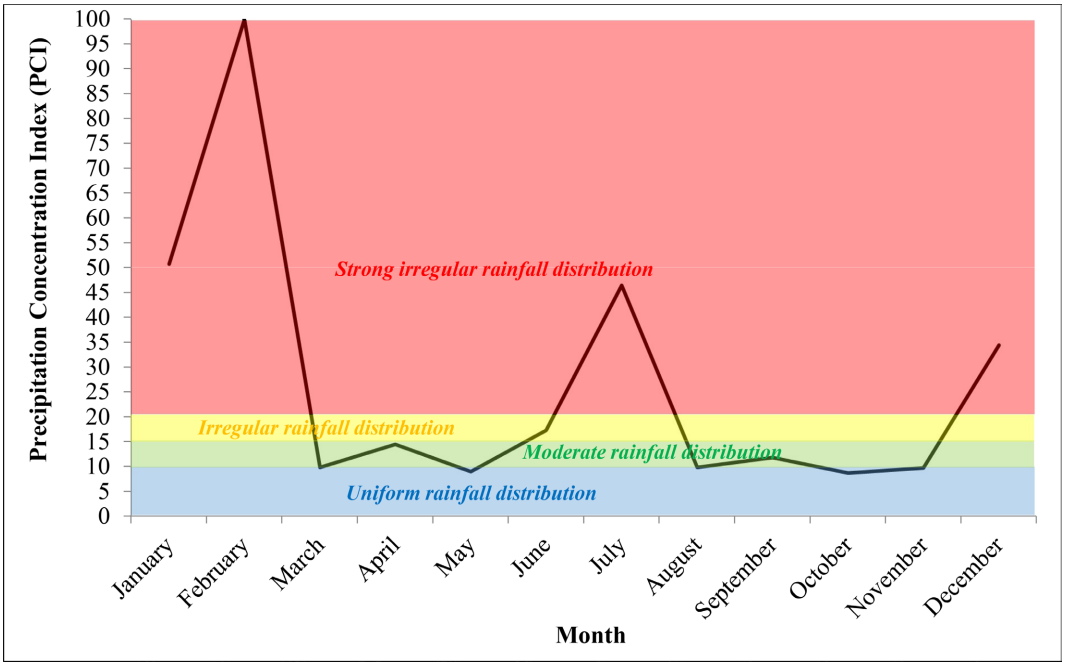

Figure 5. Monthly precipitation concentration index computed with daily rainfall data for the year 2021.

Table 3. Summary statistics of monthly precipitation trends computed with quarter-hourly daily rainfall data for the period from January 1st to December 31st 2021.

Months	Min. (mm)	Max. (mm)	Total (mm)	SD (mm)	CV (%)	Sen's slope (β)	MK Test (p-Value)	Rainfall contribution (%)	Rainfall Trends
January	0	13.6	21.4	2.69	389.98	0	−5 (0.894)	1.06	Decreasing
February	0	6.80	6.8	1.29	529.15	0	12 (0.539)	0.34	Increasing
March	0	22.4	148.2	6.97	145.74	0	65 (0.232)	7.37	Increasing
April	0	32.4	131	8.12	185.84	−0.025	−1 (0.991)	6.51	Decreasing
May	0	35.20	180.4	7.91	135.90	0.1	55 (0.358)	8.97	Increasing
June	0	50	229.4	15.94	208.43	0	30 (0.581)	11.41	Increasing
July	0	21.40	38.4	4.61	371.97	0	−68 (0.044)*	1.91	Decreasing
August	0	90.40	688	32.38	145.89	2.125	137 (0.011)*	34.21	Increasing
September	0	42.60	204.4	11.06	162.28	0	24 (0.684)	10.16	Increasing
October	0	26.40	187.8	8.04	132.70	−0.167	−7 (0.918)	9.34	Decreasing
November	0	22.20	144.8	6.80	140.82	−0.018	−93 (0.106)	7.20	Decreasing
December	0	13.60	30.4	3.10	316.06	0	−94 (0.006)*	1.51	Decreasing
Annual	**0**	**31.42**	**2011**	**181.29**	**108.18**	**0.168**	**4.58**	**100**	**Increasing**

Min.: Minimum; Max.: Maximum; SD: Standard Deviation; CV: Coefficient of Variation; MK: Mann-Kendall test;* significant at 5% level of significance.

variability in the Yaounde urban area during the year 2021 (Table 3). On the other hand, the CV of the intra-monthly daily rainfall variability was generally very high and the months of January (389.98%), February (529.15%), July (371.97%) and December (316.06%) had the highest rainfall variation.

The MK trend test showed that there was a statistically significant increase in rainfall trend for the month of August at a 5% level of significance, while a significant decreasing trend was observed in July and December (Table 3). There was no significant increase in rainfall trend that was observed in February, March, May, June and September whereas no significant decreasing trend was observed in January, April, October and November. The monthly share of rainfall exhibited about 72.46% positive trend and 27.54% negative trend in rainfall amounts.

3.1.2. Analysis of Temperature and Insolation Trends

Figure 6 gives the daily value of air temperature alongside with the polynomial regression fit of temperature distribution in the Yaounde urban area for the period from January 1st to December 31st 2021. It results from the analysis that the lowest daily mean temperature values were recorded on Saturday 20th March (20.86˚C) and Sunday 10th October (20.87˚C), whereas the highest were registered on Wednesday 3rd March (27.17˚C) and Sunday 28th February (27.02˚C). Polynomial regression analysis shows a 6th degree significant nonlinear variation

of air temperature during the year 2021, with a fairly good coefficient of determination (R^2 = 0.488) which indicates the degree to which the polynomial fit describes the data. Indeed, temperatures were generally high during the great dry season as expected, except for the small dry season (July) where values were abnormally low. The fitted model shows that temperatures are slightly related to the time scale (days) factor. The relationship seems not to be great because the seasonal nature trend of temperature was not fully depicted.

Figure 7 shows the monthly variation of the monthly mean daily minimum,

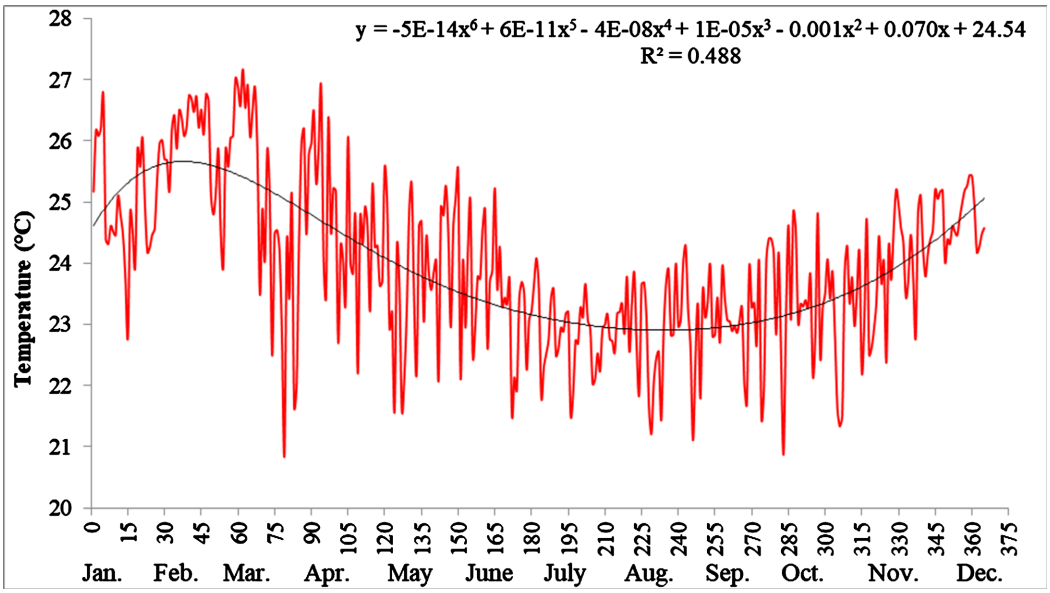

Figure 6. Daily time series of air temperature of the Yaounde urban area for the period from January 1st to December 31st 2021 and Dark line depicts the sixth order polynomial regression fit of the data.

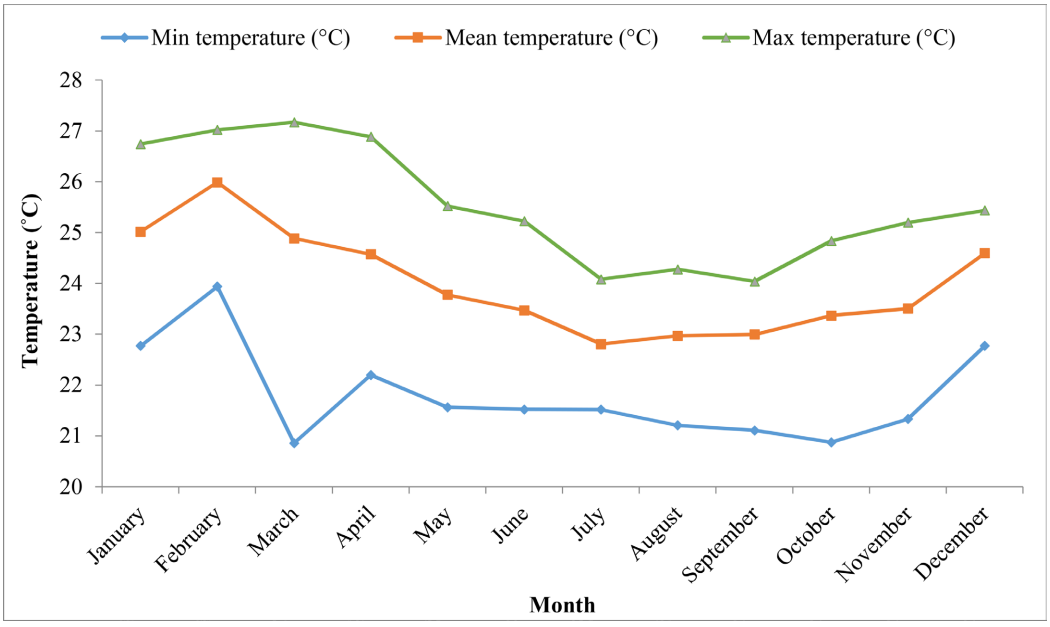

Figure 7. Monthly variation of the daily mean minimum, maximum and average values of temperature in the Yaounde urban area during the year 2021.

maximum, and average temperatures for the Yaounde urban area during 2021. The results show that the temperature values are generally higher for December through April, and lower for May through November.

Figure 8 depicts the daily values of insolation along with a sixth order polynomial regression fit for the data of Yaounde urban area during the study period, which is included to depict a smoothed evolution of the time series.

The mean annual insolation computed from quarter-hourly data in the study area for the year 2021 was 174.64 W/m^2, while the mean minimum and mean maximum value of insolation were 84.37 W/m^2 and 249.87 W/m^2 respectively (Figure 9). The monthly variation of the daily mean minimum insolation extended from 49.75 W/m^2 (March) to 124.33 W/m^2 (April). On the other hand, the mean maximum temperatures fluctuated between 207.96 W/m^2 (July) and 291.84 W/m^2 (April), whereas the monthly average values varied from 138.77 W/m^2 (July) to 206.18 W/m^2 (April).

Figure 10 shows non-overlapping 10-day averaged (dekadal) values of insolation and temperature and their covarying relationship in the Yaounde urban area data for the study period. The dekadal values of insolation and temperature were comprised between 129.82 W/m^2 (2nd dekad, July) and 221.61 W/m^2 (1st dekad, April), and between 22.48˚C (2nd dekad, August) and 26.28˚C (1st dekad, March), respectively. Except for the period between the third dekad of January and the first dekad of March where the temperature curve is overlapping that of insolation, the two trend profiles are nearly super-imposable with a general decreasing tendency from the first dekad of April to the second dekad of August, followed by new increasing trends up to the end of December.

Simple linear regression model was used to describe how strong the relationship

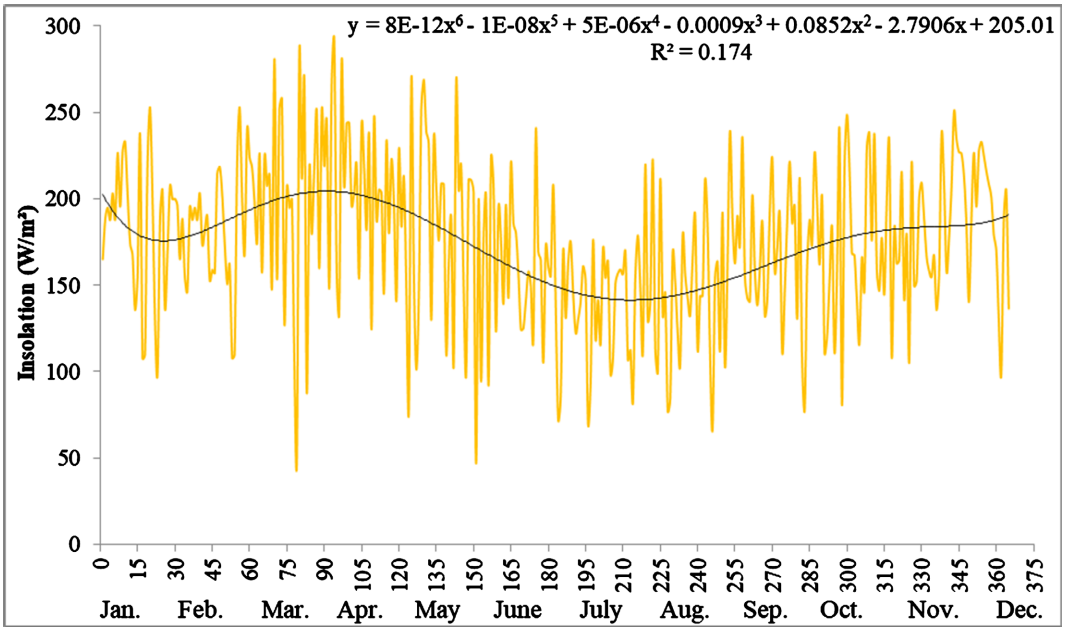

Figure 8. Daily time series of insolation of the Yaounde urban area for the period from January 1st to December 31st 2021 and Dark line depicts the sixth order polynomial regression fit of the data.

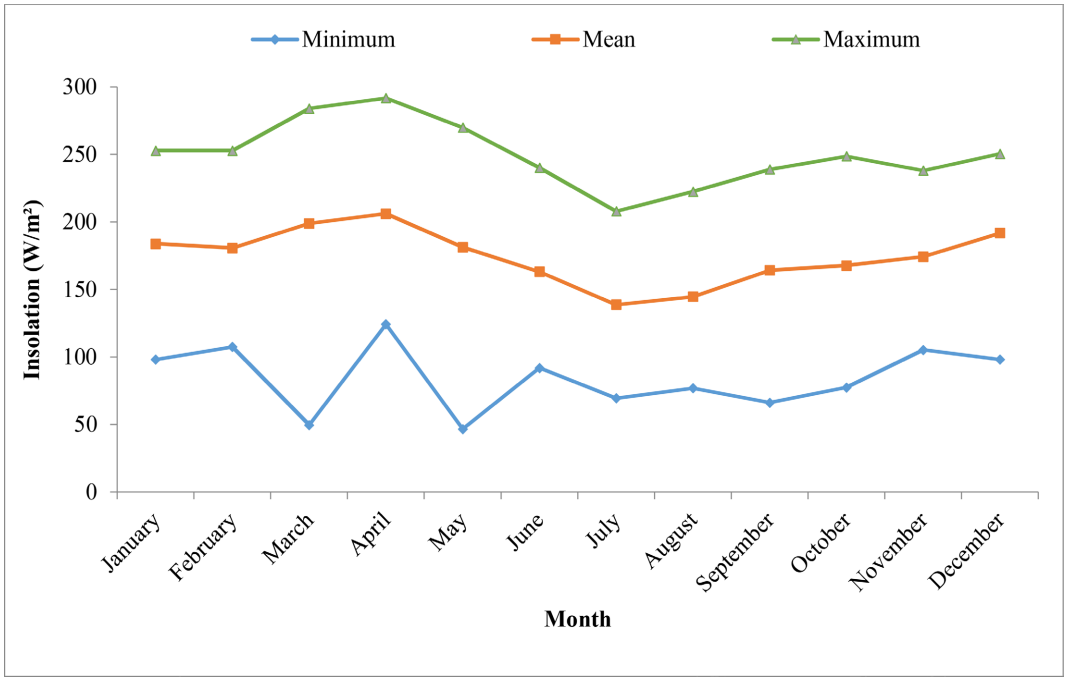

Figure 9. Monthly variation of the minimum, maximum and average values of insolation in the Yaounde urban area during the year 2021.

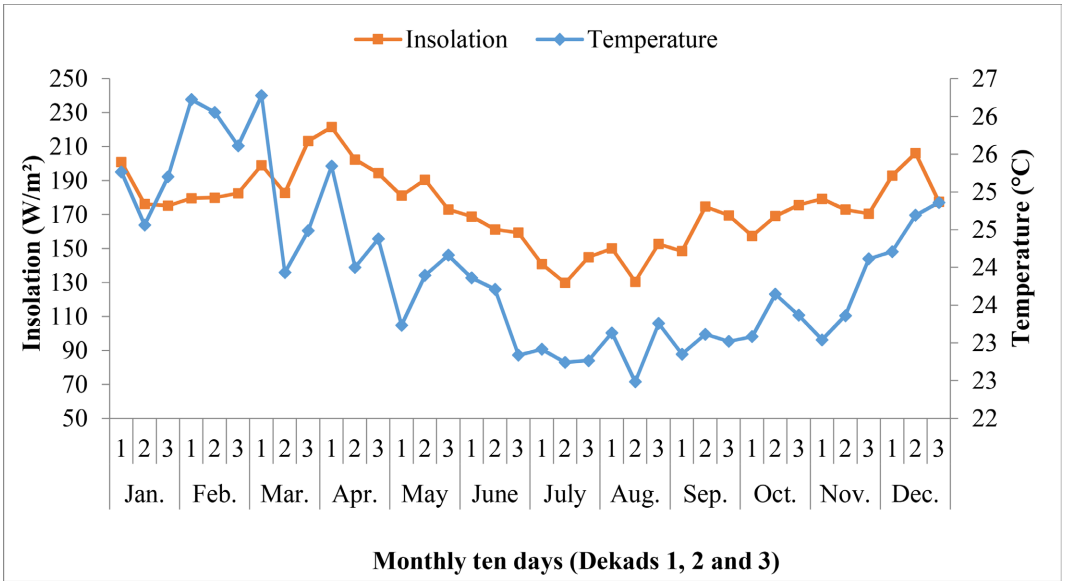

Figure 10. Average dekadal values of insolation and temperature in the Yaounde urban area for the year 2021.

is between temperature (dependent variable) and insolation (independent variable). Here, temperature is presumed to be in a linear relationship ($y = ax + b$) with the changes in insolation. Figure 11 reveals a positive and significant relationship (r = 0.704) between temperature and insolation, and a fairly good coefficient of determination ($R^2 = 0.476$).

3.1.3. Analysis of Relative Humidity and Dew Point Temperature Trends

The dew point temperature (DPT) is the temperature the air needs to be cooled

to (at constant pressure) in order to become saturated with water vapour. Figure 12 presents the daily values of relative humidity (RH, in %) and dew point temperature (DPT, in ˚C) in the Yaounde urban area during the study period. The DPT and RH time series have a Spearman correlation coefficient of r = 0.71, indicating that they covary to some degree. All of the lowest RH values were recorded during dry season whereas the highest were obtained during rainy season. Concerning the DPT trend, the curve almost overlapped that of RH during dry seasons.

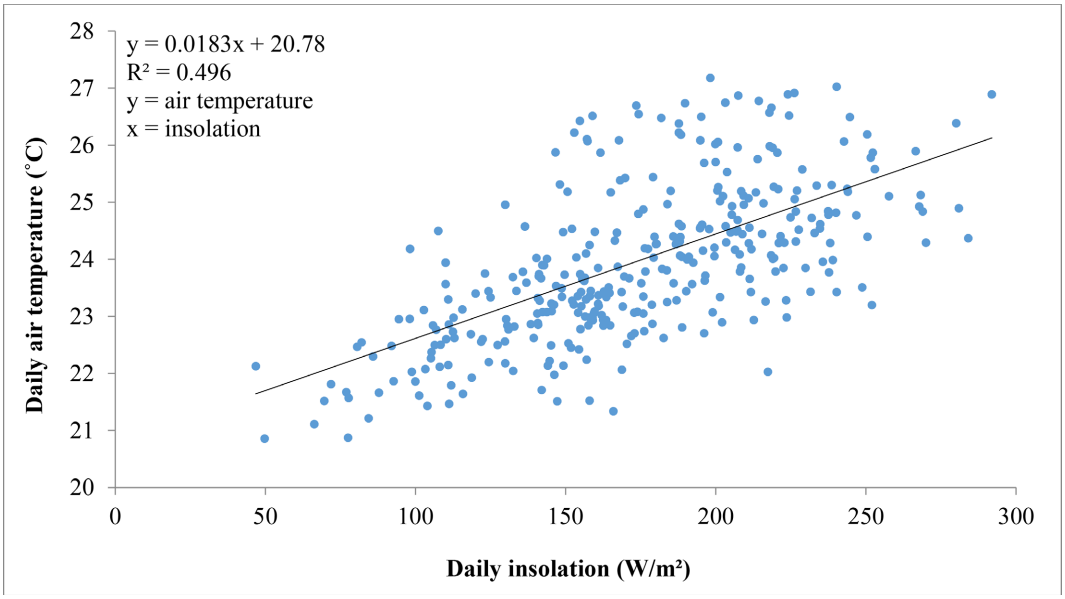

Figure 11. Linear regression showing the relationship between air temperature and insolation computed from hourly data recorded in the Yaounde urban area for the year 2021.

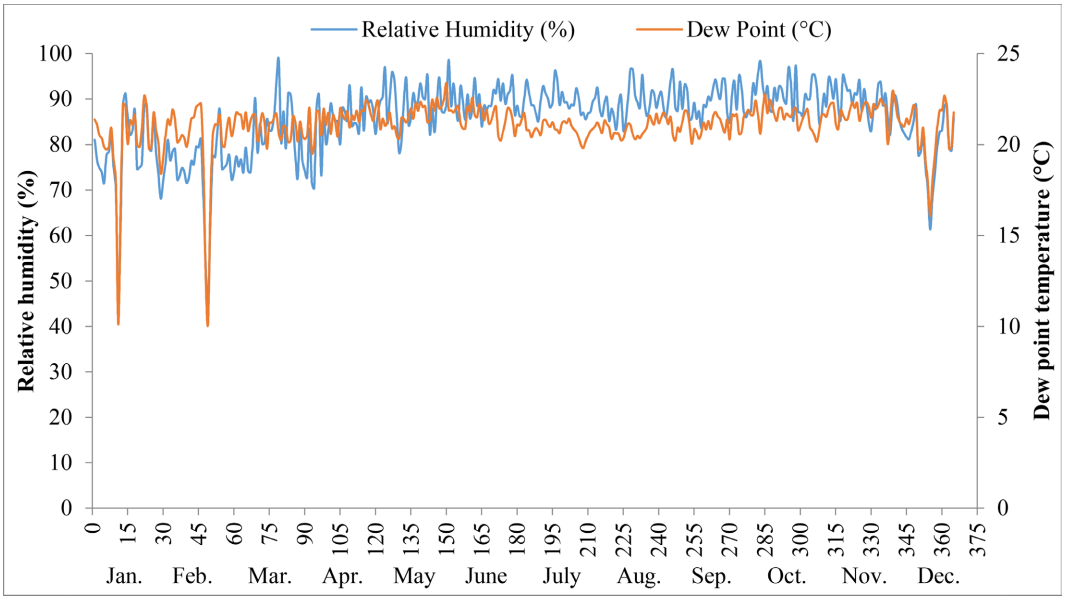

Figure 12. Daily trend graph for Relative Humidity (%) and Dew Point Temperature (˚C) of the Yaounde urban area for the period from January 1st to December 31st 2021.

3.1.4. Analysis of Wind Speed Trends

Figure 13 depicts daily mean values of wind speed together with a 6th order polynomial fit used to illustrate the gradual time-evolution of winds in the Yaounde urban area during the study period. It results from the analysis that the lowest daily mean wind speed values were recorded on Friday 14th May (0.07 km/h), Wednesday 8th September (0.16 km/h) and Tuesday 9th November (0.16 km/h), whereas the highest were registered on Saturday 2nd January (6.38 km/h), Thursday 25th February (6.38 km/h) and Tuesday 6th April (6.25 km/h). A 6th degree polynomial regression analysis shows a significant nonlinear variation of wind speed during the year 2021, with a fairly good coefficient of determination ($R^2 = 0.413$) which indicates the degree to which the polynomial fit describes the data.

3.2. Dekadal (10-Day Periods) Weather Forecasts in Yaounde in 2021 by the National Observatory on Climate Change (NOCC)

The dekadal climate early warning bulletins for the year 2021 based on historical average temperature and rainfall data from 1979 to 2018 were done by the Cameroon National Observatory on Climate Change (NOCC) through the exploitation of spatial data collected from major international centres involved in day-to-day climate science, notably: the International Research Institute for Climate and Society (IRI) of the University of Columbia (USA); the National Oceanic and Atmospheric Administration (NOAA,USA); the American Weather Forecasting Agency (AccuWeather, USA); the African Centre of Meteorological Applications for Development (ACMAD). Additionally, quarter-hourly climate data for the year 2021 were collected from the Yaounde city meteorological stations. A dekadal synthesis analysis of the historical and forecast rainfalls, maximum and

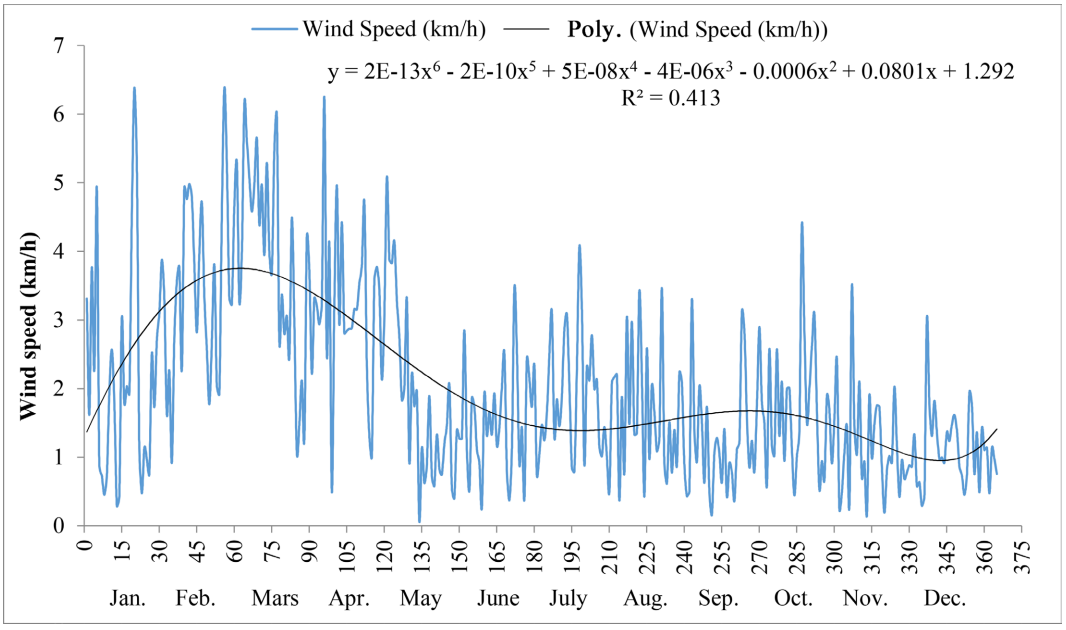

Figure 13. Daily time series of wind speed of the Yaounde urban area for the period from January 1st to December 31st 2021 and Dark line depicts the sixth order polynomial regression fit of the data.

minimum temperature averages was done and compared to the quarter-hourly data recorded throughout the year 2021 (Table 4; Figure 14 and Figure 15).

Based on the historical data from 1979 to 2018 in the bimodal rainfall forest zone, the forecast for the three dekads of January 2021 (1 - 10, 11 - 20 and 21 - 31) indicated the extension of the great dry season in the Centre region, following the influence of the Harmattan and characterised by a scarcity in rainfall. Due to the quasi-permanence of the Harmattan with more dry, cold and dusty winds, all the three dekads of February 2021 (1 - 10; 11 - 20; 21 - 28) were announced to be characterised by more aridity over the national territory (including Yaounde) with the scarcity of rainfall. However, it should be noted that the third dekad (21 - 28 February 2021) could be marked by some sporadic and localised rainfall in the southern part of the Centre region.

The dekad from 1st to 10th March 2021 was forecasted to be characterised by the extension of the great dry season and rainfall scarcity in the Centre region, following the influence of the Harmattan. For the second dekad (11 - 20 March 2021), effective start of the small rainy season was expected in the Centre region, with rainfall amounts much higher than those recorded during the first dekad. Whereas during the third dekad (21 - 30 March 2021), rainfall amounts were forecasted to decrease below those recorded during the second dekad.

Despite the effective start of the small rainy season, the period from 1st to 10th April 2021 was expected to be marked by a significant decrease in rainfall amounts compared to the average rainfall recorded in the dekads from 11th to 20th March and 21st to 30th March 2021. The period from 11th to 20th April 2021 was forecasted to be characterised by a return of normal rainfall amounts, after a significant decrease during the period from 11th March to 10th April 2021. Whereas during the third dekad (21 - 31 April 2021), rainfall amounts were expected to increase above those recorded during the second dekad.

The first and third dekads of May 2021 were predicted to show a general increase in rainfall amounts in the bimodal rainfall forest zone (including Yaounde). Inversely, for the second dekad, 11th to 20th May 2021 forecast trends predicted a general decrease in rainfall amounts. Despite the gradual onset of the small dry season as from the second dekad of June, the period from 1st to 30th June 2021 was expected to be marked by a significant and continuous increase in rainfall amounts compared to the average rainfall recorded in May 2021. Significant risk of landslides due to water logging and flooding was predicted for the third dekad (21 - 30 June 2021) in different zones of Yaounde.

The period from 1st to 10th July 2021 in Yaounde was expected to be marked by a rainfall amount below the average recorded during the dekad from 21st to 30th June 2021. Likewise, the rainfall amounts obtained during the second dekad (11 - 20 July 2021) were predicted to fall below the average recorded during the dekad from 1st to 10th July 2021. Contrariwise, the rainfall concentration predicted for the third dekad (21 - 30 July 2021) was to be around the average recorded during the second dekad.

Table 4. Dekadal (10-day periods) weather anomalies in Yaounde in 2021 based on the historical averages for the period from 1979 to 2018.

Dekads	Historical average temperatures (˚C) from 1979 to 2018		Temperatures (˚C) recorded in 2021			Historical mean rainfall (1979 to 2018)	Recorded total rainfall in 2021
	Min.	Max.	Min.	Max.	Average		
Jan. 1	19	29	20.76↗	32.56↗	25.27	4.7	0↘
Jan. 2	19.5	29.5	20.22↗	31.37↗	24.56	5.6	21.4↗
Jan. 3	20	30	20.91↗	31.76↗	25.2	6.5	0↘
Feb. 1	19.9	30	21.93↗	32.74↗	26.23	8.1	0↘
Feb. 2	19.5	29.3	21.5↗	32.2↗	26.06	10.3	0↘
Feb. 3	20	29	21.43↗	32.46↗	25.61	17.1	6.8↘
Mar. 1	20	29	21.77↗	33.48↗	26.28	25.1	36.4↗
Mar. 2	19.4	29.5	19.96↗	31.42↗	23.93	37.7	61.4↗
Mar. 3	23	32.6	20.45↘	31.1↘	24.49	51.2	50.4↘
Apr. 1	19	30	21.01↗	32.04↗	25.34	56.1	16.6↘
Apr. 2	19	29.3	19.78↗	30.81↗	24	64.4	82.6↗
Apr. 3	19	29	20.69↗	31.2↗	24.38	51.3	31.8↗
May. 1	20.7	29.6	19.61↘	29.91↗	23.24	59.7	52.6↘
May. 2	20	28.1	20.24↗	29.53↗	23.9	59.1	63↗
May. 3	19	27.8	20.25↗	29.52↗	24.16	61.7	64.8↗
Jun. 1	19	28	20.45↗	29.44↗	23.86	44.6	54↗
Jun. 2	19	28	20.48↗	29.28↗	23.71	45.6	54.8↗
Jun. 3	19	28	19.79↗	28.19↗	22.84	47.3	120.6↗
Jul. 1	19	27.53	20.11↗	27.56↗	22.92	39.6	23↘
Jul. 2	19	27	20.34↗	26.92↘	22.74	33.5	15.4↘
Jul. 3	19	27	19.91↗	27.08↗	22.77	47.3	0↘
Aug. 1	19.4	27	20.4↗	28.03↗	23.13	41.8	1.8↘
Aug. 2	19.4	27	19.8↗	27.71↗	22.48	52.9	268.8↗
Aug. 3	19.4	27	20.3↗	29.28↗	23.26	65.1	417.4↗
Sep. 1	20.7	27	19.92↘	28.74↗	22.85	69.6	49↘
Sep. 2	20.4	27	19.63↘	28.93↗	23.12	76.1	40.2↘
Sep. 3	20.1	27	19.95↘	28.61↗	23.02	81.9	115.2↗
Oct. 1	18	27	19.7↗	28.62↗	23.08	76.4	88↗
Oct. 2	19.6	27	19.96↗	29.23↗	23.65	94.8	30.8↘
Oct. 3	19	27	19.93↗	29.04↗	23.37	97.6	69↘
Nov. 1	19.2	28	19.46↗	28.65↗	23.04	71.8	44.2↘
Nov. 2	20.1	28	19.93↘	28.69↗	23.36	37.6	73↗
Nov. 3	18.6	28	20.15↗	29.64↗	24.12	20.9	27.6↗
Dec. 1	20.5	28	19.91↘	29.38↗	24.21	14.7	30.4↗
Dec. 2	18.9	28	20.53↗	29.79↗	24.69	6.82	0↘
Dec. 3	19	28	20.8↗	30.26↗	24.86	5.71	0↘

Legend: ↗ *increase trend;* ↘ *decrease trend*

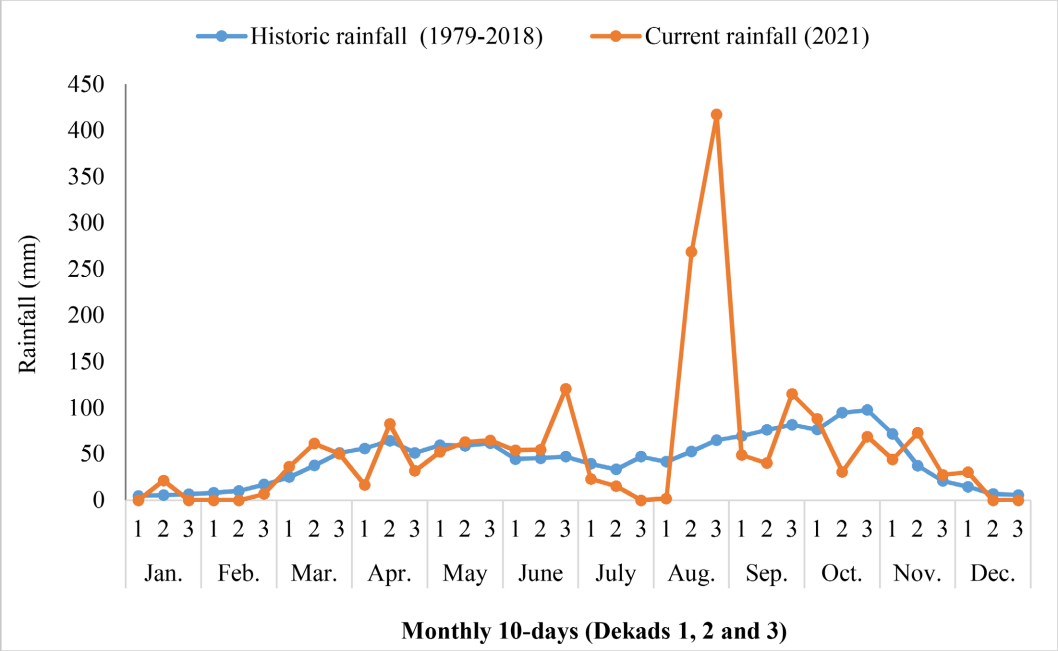

Figure 14. Dekadal variation of historical mean rainfall (from 1979 to 2018) and rainfall recorded during the year 2021 in the Yaounde urban area.

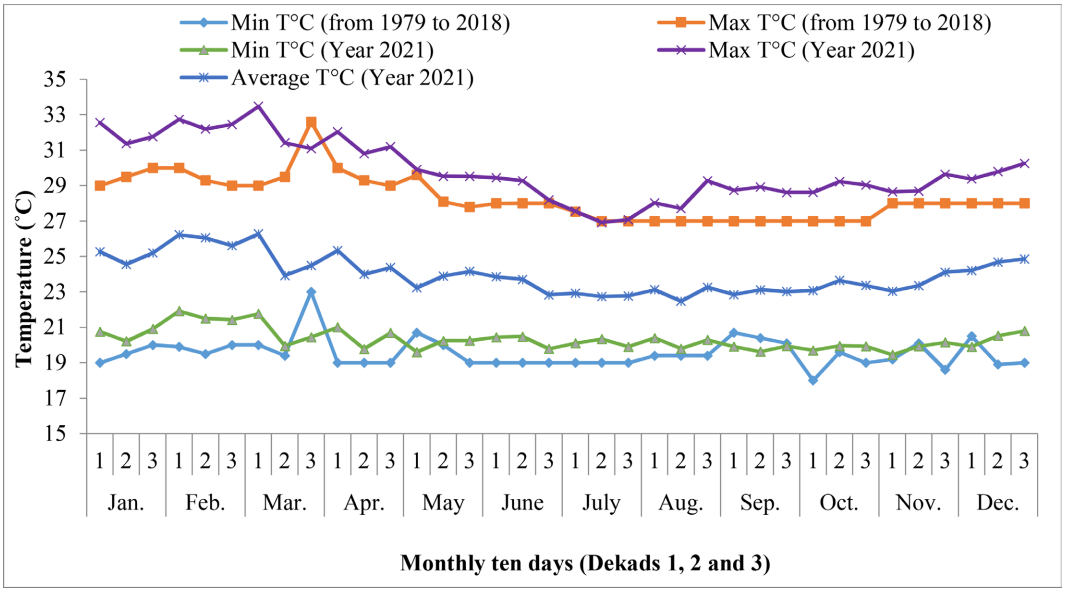

Figure 15. Comparative dekadal trends of the historical (from 1979 to 2018) and year 2021 maximum and minimum temperature averages recorded in the Yaounde urban area.

All the three dekads of August 2021 were considered to correspond to the continuation of the short dry season in Yaounde, marked by very low rainfall amounts, expected to be slightly above the average recorded during the dekad from 21st to 30th July 2021.

The dekad from 1st to 10th September 2021 is marked by the effective start of the great rainy season in the bimodal rainfall forest zone (including Yaounde) with abundant rainfall. It was predicted that rainfall amounts during this first

dekad were to increase significantly above the average recorded during the dekad from 21st to 30th August 2021. Likewise, the rainfall amounts obtained during the second dekad (11 - 20 September 2021) were predicted to increase slightly above the average recorded during the dekad from 1st to 10th September 2021. The third dekad (21 - 30 September 2021) correspond to the continuation of the great rainy season, with significant rainfall and high risk of flooding and landslides due to water logging in Yaounde.

All over the three dekads of October 2021, the continuation of the great rainy season was predicted in Yaounde, with more abundant rainfall. The rainfall amounts were to increase significantly above the average recorded during the dekad from 21st to 30th September 2021, with significant rainfall and high risk of flooding and landslides due to water logging.

The dekad from 1st to 10th November 2021 is marked by the continuation of the great rainy season with nevertheless decreasing rainfall amounts. Likewise, during the dekad from 11th to 20th November 2021, rainfall amounts were predicted to decrease below the average recorded during the first dekad. The third dekad (21 - 30 November 2021) corresponds to the gradual onset of the great dry season characterised by a scarcity in rainfall. The general decrease in rainfall amounts is an indicator of the shift towards the end of the great rainy season and the beginning of the great dry season in this agro-ecological region.

All the three dekads of December 2021 were predicted to be marked by the gradual and effective onset of the great dry season in the Centre region, reflected by an increasing scarcity of rainfall although some sporadic and low intensity light rains could be observed in Yaounde.

Figure 14 highlights the Dekadal variation of historical mean rainfall (1979-2018) and rainfall recorded during the year 2021 in the Yaounde urban area. It results from the graph that rainfalls were generally higher in the small rainy season (from March to June) during the year 2021 compared to historical averages in the same locality, except for the 1st and 3rd dekads of April, and the 1st dekad of May. During the great rainy season (from August to November) unevenly high rainfall values were recorded during the 2nd and 3rd dekads of August 2021.

To determine the intensity and direction of shift in temperature, the differences of mean maximum and minimum temperature values between the year 2021 and historical (1979-2018) data were computed (Figure 16). Comparative to historical data, the 2021 temperature witnessed an annual mean increase of 0.80˚C and 1.58˚C for mean minimum and mean maximum respectively. Indeed, except for the third dekad of March (−1.5˚C) and second dekad of July (−0.08˚C), all the mean maximum temperatures differences were above zero, indicating an increase. Concerning mean minimum temperature differences, just 7 dekads (19.44%) recorded negative values whereas the 29 remainders (80.56%) have values above zero, indicating an overall increase.

3.3. Relationship between Weather Metrics and Flood Events

In addition to geographical location and anthropogenic land use/land cover

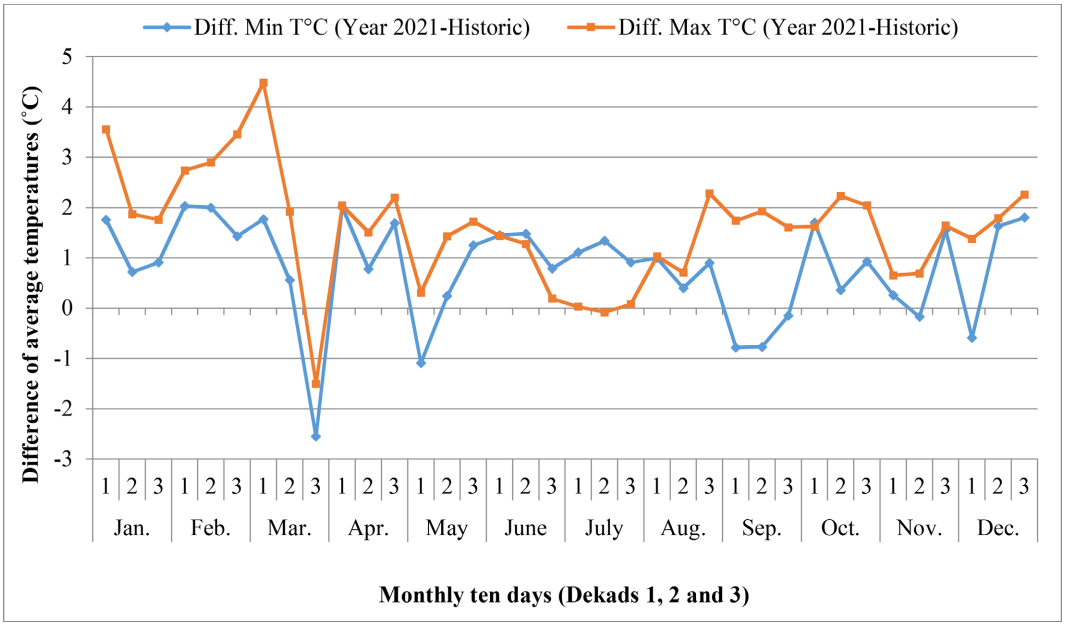

Figure 16. Graphical trend of the average maximum and minimum temperature differences between the data of year 2021 and the historical data (from 1979 to 2018).

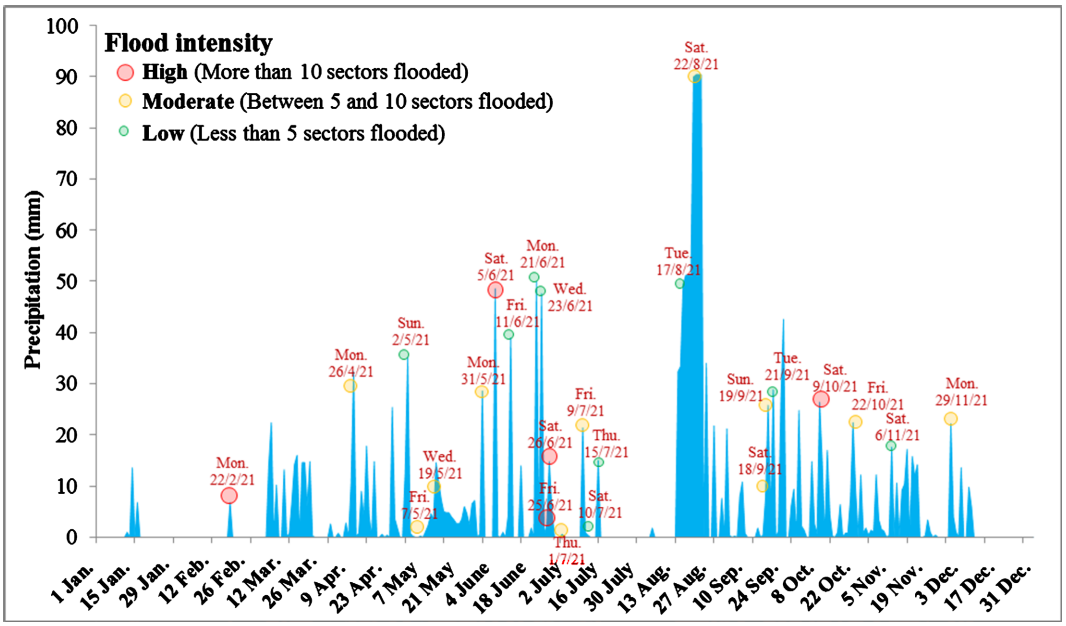

Figure 17. Daily rainfall variation curve in Yaounde in 2021 showing flooded days and flood's intensity.

changes that alter water flow regimes, flood events are closely linked to rainfall intensity, duration and frequency. Figure 17 highlights the flooded days and flood's intensity observed in Yaounde in 2021. Overall, 25 flooded days were recorded in the study area during the study period, with the highest flood occurrence observed in June (6 flooded days) followed by May and July (4 flooded days each), September (3 flooded days), August, October and November (2 flooded days each), and finally April and February with just one flooded day each. With regards to flood intensity determined on the basis of the number of sectors regu-

larly flooded, 20% (5/25 days) of floods were classified as high, whereas 44% (11/25 days) and 36% (9/25 days) were termed as moderate and low, respectively. From Figure 17, it appears that flood intensity was not in some cases linearly correlated to the recorded rainfall amounts. Indeed, flood intensity is not solely related to rainfall amounts as the combination of other factors such as rainfall duration and distribution (i.e. the number of sectors/neighbourhoods affected by rain), geomorphology of the area and anthropogenic activities (existence, state and cleaning frequency of gutters and waterways) might explain the low to moderate flood intensity observed in some cases where high precipitation amounts were recorded, and vice versa. For instance, based on field observation, low and moderate flood intensities noticed in August 2021 were probably related on the one hand, to rainfall distribution since the heavy rainfalls of the 17th and 22nd August 2021 touched partially only the Western and Northern parts of the city of Yaounde, causing flooding just in the few affected quarters. On the other hand, these heavy rainfalls did not last for long.

Slope is one of the key factors influencing surface runoff and rainwater infiltration. Therefore, areas with low slopes are more subjected to flood because of the low surface runoff velocity, whereas those with high slopes have high runoff velocity that is incompatible with flooding (Das, 2020; Nsangou et al., 2022). The slope map of the Mfoundi basin (Map 2) is largely covered by green colour indicating that the study area is dominated by low slopes, with high concentration of flood prone zones in the central town. Among the prospected areas that were quickly and most often flooded during the study period, Kennedy Street, Central Post Office, Mfoundi Market, Ahala II and Damas MAETUR were the most repeatedly flooded sectors in 2021 (Figure 18).

As not all factors have the same degree of influence on the flood generation mechanism in a given area, it is important to assess the effect of each factor in flood occurrence. Non-parametric Spearman correlation test reveals that flood occurrence was positively and significantly related to precipitation ($r = 0.676$, $p < 0.05$), and negatively and significantly correlated to RH ($r = -0.651$, $p < 0.05$) and insolation ($r = -0.669$, $p < 0.05$). On the other hand, the number of rainy days appears to be highly significantly and positively related to precipitation ($r = 0.711$, $p < 0.01$) and DPT ($r = 0.886$, $p < 0.01$). In addition, precipitation shows a significantly positive relationship with DPT ($r = 0.734$, $p < 0.01$), and negative significant correlations with RH ($r = -0.762$, $p < 0.01$), insolation ($r = -0.601$, $p < 0.05$) and wind speed ($r = -0.643$, $p < 0.05$).

4. Discussion

Results of this study revealed that the total rainfall (2011 mm) and average temperature (24˚C ± 1˚C) recorded in Yaounde during the year 2021 were far above the historical annual averages of rainfall (1554 ± 261 mm) and temperature (23.5˚C) registered in the same area between 1964 and 2019 (Nsangou et al., 2022). These results are in contradiction with the study by Zogning (2017) which

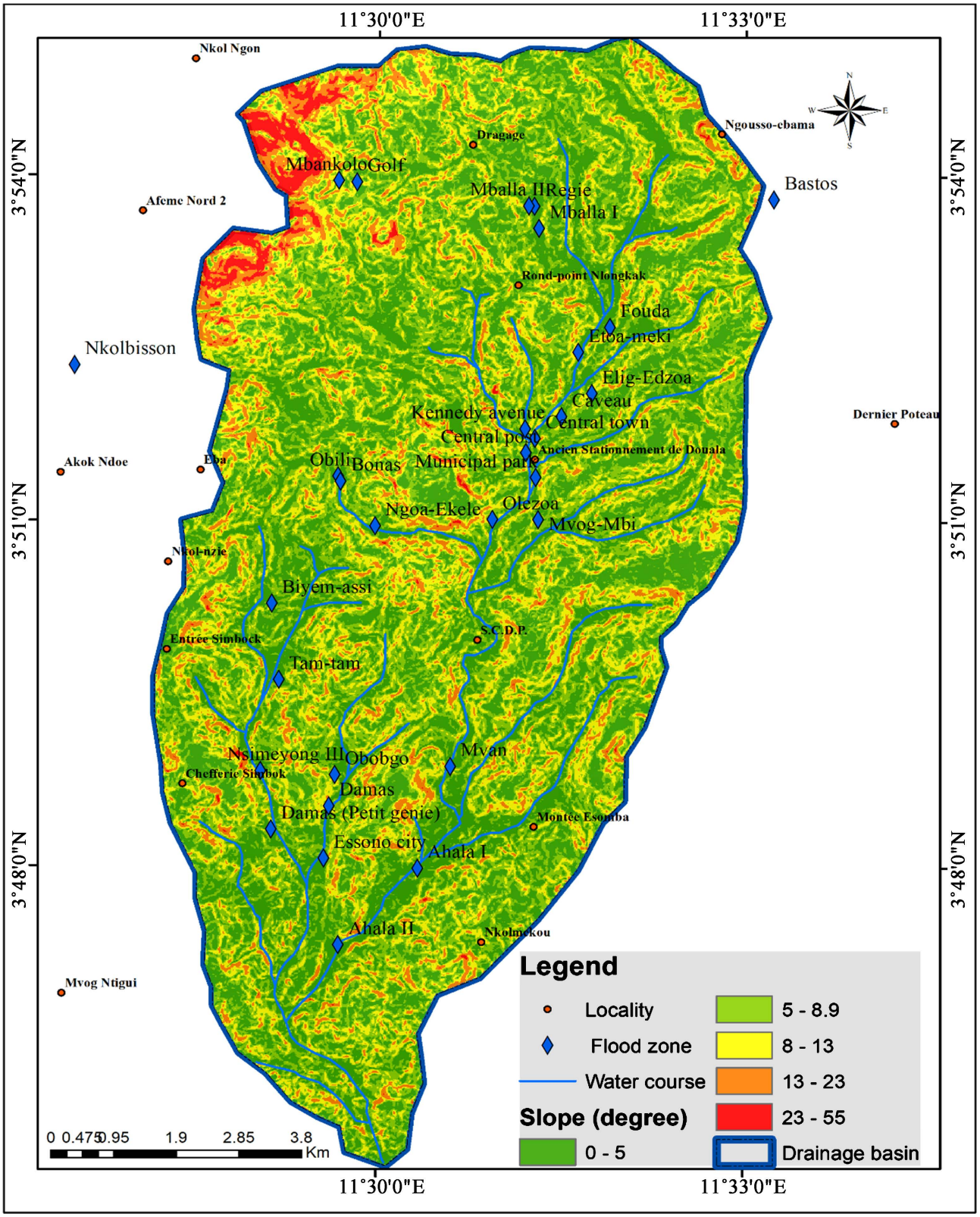

Map 2. Slope map of the Mfoundi watershed including the most 30 frequently flooded points identified during the study period.

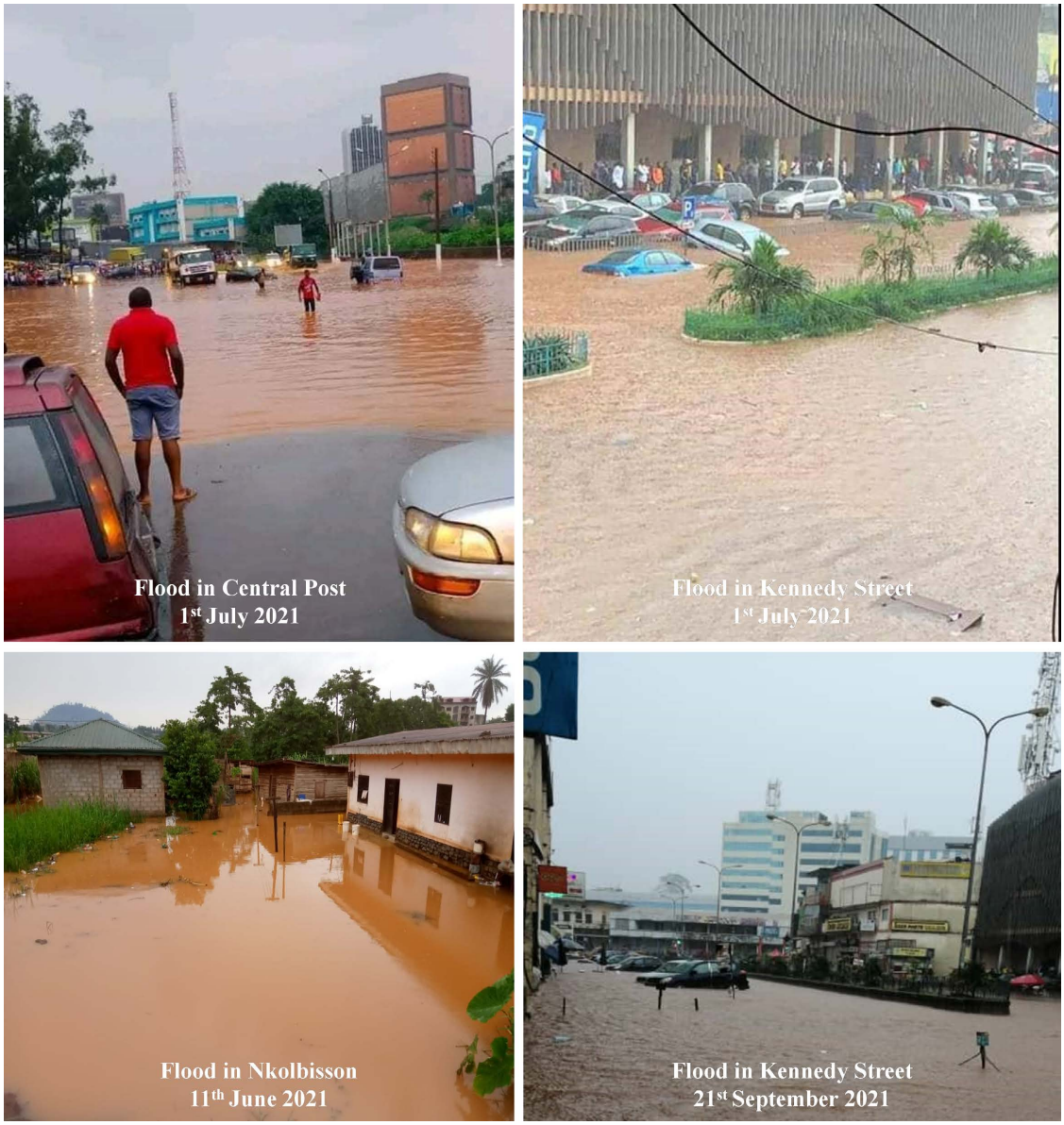

Figure 18. Partial views of some flooded areas in Yaounde in 2021. *Photo credit: Nimpa Tatiana.*

showed a 9.2% reduction in rainfall within the period 1970-2016 in Yaounde, and concluded that similar trends were to be observed for upcoming years. Strong irregular rainfall distributions were observed between seasons and within the rainy seasons, with the highest total rainfall being historically recorded in August 2021 (688 mm). This significant increase in rainfall is statistically confirmed by the MK trend test. Indeed, during the year 2021, the city of Yaounde was marked by unusual high rainfall especially in August, and much more frequent rainy days during dry seasons. These results differ from those of previous authors who showed that historically in Yaounde, higher monthly average rainfall values were recorded in September and October (Guenang & Kamga, 2014; Zogning, 2017; Nsangou et al., 2022). Concerning temperature analysis, the dekadal minimum and maximum values recorded in Yaounde in 2021 were

generally higher than the forecasted values based on the historical averages for the period from 1979 to 2018. Similar increases in temperature have been recorded in previous studies in the same area (Guenang & Kamga, 2014; Zogning et al., 2016; Zogning, 2017; Nsangou et al., 2022). Despite the overall increase in temperature observed in the study area, rainfalls were still abundant and regular with a total of 161 rainy days registered in 2021. This number of rainy days is greater than the historical annual average values (148.8 days/year) reported in Yaounde by (Zogning, 2017) for the period 1951-2015. Our results are similar to those of Namondo et al. (2022) who showed that although the prolonged dry season there were still abundant rainfalls causing historical flood disastrous events in many neighbourhoods in Limbe (South-West Region). A similar study was carried out in the city of Bamenda (Saha & Tchindjang, 2017) and concluded that extreme flood events will occur more frequently due to changes and variability in climate as it is the case observed in Yaounde.

Values of SPI which showed that the weather was generally wetted (from mildly to extremely wetted) both during dry and rainy seasons are in line with RH values which were generally high with an average of 85.76%. Spearman correlation test shows significant positive relationship between RH and dew point, which are important elements in determining rainfall distribution, with dew point temperatures being higher when air contains greater amounts of water vapour. Tabari (2020) documented that water availability also plays a large role in the moisture-temperature relationship. Our results are in line with those revealed by Fotso-Nguemo et al. (2017) which showed that future rainfall over High Lands of Cameroon (including the city of Yaounde), Adamawa Plateau, North-eastern Democratic Republic of Congo and Atlantic Ocean is projected to increase. Values of PCI revealed that rainfalls were either uniformly (5/12 months, i.e. 41.67%) or moderately (2/12 months, i.e. 16.67%) distributed during rainy seasons, indicating constant and frequent rainfalls. According to Ingram (2016) and IPCC (2021), extreme precipitation is expected to intensify with global warming over large parts of the globe as the concentration of atmospheric water vapour which supplies the water for precipitation increases in proportion to the saturation concentrations.

Concerning flood occurrence in Yaounde, the major sensitive flood prone areas we monitored witness flooding during 25 days all over the year 2021; no flood being observed in December, January and March on these monitoring sites. Kennedy Street, Central Post Office, Mfoundi Market, Ahala II and Damas MAETUR were the most repeatedly flooded sectors. Similar results were obtained by previous authors (Zogning et al., 2011, 2016; Nsangou et al., 2022; Onana et al., 2022) who pointed out Kennedy Street and Central Post Office as the most frequently and easily flooded areas in the Yaounde urban area. Moreover, Spearman correlation test reveals strong and significant relationship between flood occurrence and climate data in Yaounde. By adding climate factors to the list of major causes of flooding in Yaounde, this study complemented that of Zogning et al. (2011) who concluded that human factors (urban growth) were the main causes of floods in Yaounde. However, the IPCC (2022) reported that

temperatures have increased above natural variability and that the frequency and intensity of heavy precipitation events leading to floods were likely to increase in the Central African region due to climate change. In the study of climate change impact on extreme precipitation and flood intensities, Tabari (2020) revealed an intensification of extreme precipitation and flooding events over all climate regions which increases as water availability increases from dry to wet regions. Similarly, there is an increase in the intensification of extreme precipitation and flooding with the seasonal cycle of water availability.

5. Conclusion

This study aimed at analyzing weather anomalies to assess the 2021 flood patterns in Yaounde. Flood is a result of many conditions working singly and in synergy. Warmer temperatures increase evaporation, putting more moisture into the atmosphere that then gets released as rain. In addition to the hydrological, geomorphological and anthropogenic characteristics of the adjoining watershed, flooding is also closely linked to rainfall intensity, duration and frequency; this exacerbates frequency and intensity of extreme flood events. Results of this study relating weather variations to flooding in Yaounde clearly matched flood occurrences to rainy days with high rainfall values. Also, flood intensity was not at all points linearly correlated to the amount of rainfall recorded. Analyses of weather anomalies from the study site therefore revealed that flood intensity was not solely related to rainfall amount and it is suggested that other factors such as rainfall distribution, geomorphology of the area and anthropogenic activities could have played a significant role. The analyses revealed that the city of Yaounde witnessed more than 25 flood events in various neighbourhoods with many socio-economic and environmental damages. With regard to abnormal rainy days, flooding events were recorded as well in many neighbourhoods of Yaounde, both during dry and rainy seasons. The strong irregular flood events recorded were for instance during the months of July and August 2021. Abundant flood events were recorded during the months of June, July, August, and September. The overall trends of some weather parameters particularly temperature and rainfall are increasing (IPCC, 2023; Fotso-Nguemo et al., 2017). It is very urgent that the Cameroonian government achieves the Yaounde Water Management and Treatment Project (PADY) in order to reduce flood occurrence in Yaounde in the context of climate change. Also, the findings from this study can be used by stakeholders involved in decision-making to take appropriate measures and interventions to avert the risks posed by changes in weather factors in order to enhance community adaptation, mitigation and resilience strategies to face floods in Yaounde.

Acknowledgements

Authors gratefully acknowledged AUF (Agence Universitaire de la Francophonie) and its partners SCAC (Service d'Action Culturelle des Ambassades de France au Cameroun) and IRD (Institut de Recherche pour le Développement)

for the South-North mobility grant awarded to the first author. We also express our gratitude to Image, City and Environment Laboratory (LIVE) at the Faculty of Geography and Planning of the University of Strasbourg, France and particularly to Dr Florentin BRETON for the traineeship granted to the first author on the analysis of climate change factors.

Conflicts of Interest

The authors declare no conflicts of interest regarding the publication of this paper.

References

Asfaw, A., Simane, B., Hassen, A., & Bantider, A. (2018). Variability and Time Series Trend Analysis of Rainfall and Temperature in North Central Ethiopia: A Case Study in Woleka Sub-Basin. *Weather and Climate Extremes, 19,* 29-41. https://doi.org/10.1016/j.wace.2017.12.002

Assako Assako, R. J. (1997). Apport des systèmes d'information géographique dans l'analyse des risques d'inondation et de glissement de terrain à Yaounde1. In D. Bley, J. Champaud, P. Baudot, B. Brun, H. Pagezy, & N. Vernazza-Licht (Eds.), *Villes du Sud et environnement, Travaux de la société d'écologie humaine* (pp. 110-124). Bergier.

Birsan, M. V., Molnar, P., Burlando, P., & Pfaundler, M. (2005). Stream Flow Trends in Switzerland. *Journal of Hydrology, 314,* 312-329. https://doi.org/10.1016/j.jhydrol.2005.06.008

Das, S. (2020). Flood Susceptibility Mapping of the Western Ghat Coastal Belt Using Multi-Source Geospatial Data and Analytical Hierarchy Process (AHP). *Remote Sensing Application: Society and Environment, 20,* Article ID: 100379. https://doi.org/10.1016/j.rsase.2020.100379

De Luis, M., Raventós, J., González-Hidalgo, J., Sánchez, J., & Cortina, J. (2000). Spatial Analysis of Rainfall Trends in the Region of Valencia (East Spain). *International Journal of Climatology, 20,* 1451-1469. https://doi.org/10.1002/1097-0088(200010)20:12<1451::AID-JOC547>3.0.CO;2-0

Djiangoué, B. (2017). Inondations et vulnérabilité des systèmes de production agricole: Cas du Logone (Extrême-Nord) et de la Bénoué (Nord) Cameroun. In N. K. Liba'a, B. Djiangoué, & W. C. Mvo (Eds.), *Risques et catastrophes en zone Soudano-Sahelienne du Cameroun: Entre aléas, vulnérabilités et résiliences* (pp 35-53). Editions Cheikh Anta Diop (Edi-CAD).

Ebode, V. B. (2022). Hydrological Variability and Flood Risk in a Forest Watershed Undergoing Accelerated Urbanization: The Case of Mefou (South Cameroon). *Water Supply, 22,* 8778-8794. https://doi.org/10.2166/ws.2022.398

Esayas, B., Simane, B., Teferi, E., Ongoma, V., & Tefera, N. (2019). Climate Variability and Farmers' Perception in Southern Ethiopia. *Advances in Meteorology, 2019,* Article ID: 7341465. https://doi.org/10.1155/2019/7341465

Fotso-Nguemo, T. C., Vondou, D. A., Tchawoua, C., & Haensler, A. (2017). Assessment of Simulated Rainfall and Temperature from the Regional Climate Model REMO and Future Changes over Central Africa. *Climate Dynamics, 48,* 3685-3705. https://doi.org/10.1007/s00382-016-3294-1

Gocic, M., & Trajkovic, S. (2013). Analysis of Changes in Meteorological Variables Using Mann-Kendall and Sen's Slope Estimator Statistical Tests in Serbia. *Global and Planetary Change, 100,* 172-182. https://doi.org/10.1016/j.gloplacha.2012.10.014

Guenang, G. M., & Kamga, M. F. (2014). Computation of the Standardized Precipitation Index (SPI) and Its Use to Assess Drought Occurrences in Cameroon over Recent Decades. *Journal of Applied Meteorology and Climatology, 53,* 2310-2324. https://doi.org/10.1175/JAMC-D-14-0032.1

Hänsel, S., Schucknecht, A., & Matschullat, J. (2016). The Modified Rainfall Anomaly Index (mRAI)—Is This an Alternative to the Standardised Precipitation Index (SPI) in Evaluating Future Extreme Precipitation Characteristics? *Theoretical and Applied Climatology, 123,* 827-844. https://doi.org/10.1007/s00704-015-1389-y

Hare, W. (2003). *Assessment of Knowledge on Impacts of Climate Change-Contribution to the Specification of Art. 2 of the UNFCCC: Impacts on Ecosystems, Food Production, Water and Socio-Economic Systems*. WBGU Report, Potsdam-Berlin, Germany.

Ingram, W. (2016). Extreme Precipitation: Increases All Round. *Nature Climate Change, 6,* 443-444. https://doi.org/10.1038/nclimate2966

IPCC (2021). *Climate Change 2021: The Physical Science Basis. Contribution of Working Group I to the Sixth Assessment Report of the Intergovernmental Panel on Climate Change*. Cambridge University Press.

IPCC (2022). *Climate Change 2022: Impacts, Adaptation and Vulnerability. Contribution of Working Group II to the Sixth Assessment Report of the Intergovernmental Panel on Climate Change*. Cambridge University Press.

IPCC (2023). *The Intergovernmental Panel on Climate Change's Sixth Assessment Report (AR6), Working Group II-Climate Change 2023: Impacts, Adaptation, and Vulnerability.* IPCC Working Group II Technical Support Unit, c/o Carnegie Institution for Science, Stanford, CA 94305, USA.

Karabulut, M. (2015). Drought Analysis in Antakya-Kahramanmaraş Graben, *Turkey Journal of Arid Land, 7,* 741-754. https://doi.org/10.1007/s40333-015-0011-6

Mann, H. B. (1945). Nonparametric Tests against Trend. *The Econometric Society, 13,* 245-259. https://doi.org/10.2307/1907187

Mboka, J.-J. M., Kouna, S. B., Chouto, S., Djuidje, F. K., Nguy, E. B., Fotso-Kamga, G., Matsaguim, C. N., Fotso-Nguemo, T. C., Nghonda, J. P., Vondou, D. A., & Yepdo, Z. D. (2020). Simulated Impact of Global Warming on Extreme Rainfall Events over Cameroon during the 21st Century. *Weather, 76,* Article No. 3867. https://doi.org/10.1002/wea.3867

Mediebou, C. (2023). Les inondations dans les bas-fonds de la commune de Yaounde 6 (Centre-Cameroun): Etat des lieux et perspectives. *Revue espace géographique et société Marocaine, 69,* 1-26.

MINEPDED (2015). *Plan National d'Adaptation aux Changements Climatiques.* Rapport d'activités, Ministère de l'Environnement, de la Protection de la Nature et du Développement Durable (MINEPDED), Yaounde, Cameroun.

Namondo, F. E., Nechia, W. M., & Ndonwi, A. S. (2022). Assessing Rainfall and Temperature Trend: Implication on Flood Patterns in Vulnerable Communities of Limbe and Douala, Cameroon. *International Journal of Environmental Science, 7,* 1-13. http://www.iaras.org/iaras/journals/ijes

Nguemou, T. D. (2008). *Hydrologie et transports solides dans un écosystème forestier urbanisé: Exemple du bassin versant du Mfoundi au centre sud du Cameroun.* Mémoire DEA., Faculté des Sciences, Université de Yaounde I.

NIS (2019). *Annuaire Statistique du Cameroun: Chapitre 4: Habitat et conditions de vie*. National Institute for Statistics (NIS) Report.

Nsangou, D., Kpoumié, A., Mfonkac, Z., Ngouh, A. N., Fossi, D. H., Jourdan, C., Zobo

Mbele, H., Mouncherou, O. F., Vandervaere, J.-P., & Ndam Ngoupayou, J. R. (2022). Urban Flood Susceptibility Modelling Using AHP and GIS Approach: Case of the Mfoundi Watershed at Yaounde in the South-Cameroon Plateau. *Scientific African, 15,* e01043. https://doi.org/10.1016/j.sciaf.2021.e01043

Oliver, J. E. (1980). Monthly Precipitation Distribution: A Comparative Index. *The Professional Geographer, 32,* 300-309. https://doi.org/10.1111/j.0033-0124.1980.00300.x

Onana, N. A., Leumbe, O., Lemotio, W., Sandjong, J. K., & Kamto, P. G. (2022). Contribution to Flood Hazard Mapping in the Mfoundi Catchment in Yaounde (Cameroon) through Multi Criteria Analysis (MCA) Based on the Hierarchical Analysis Process (AHP). *Bulletin de l'Institut Scientifique, Rabat, Section Sciences de la Terre, 44,* 13-27.

Saha, F., & Tchindjang, M. (2017). Rainfall Variability and Floods Occurrence in the City of Bamenda (Northwest of Cameroon). *De Gruyter PESD, 11,* 65-82. https://doi.org/10.1515/pesd-2017-0006

Sen, P. K. (1968). Estimates of the Regression Coefficient Based on Kendall's Tau. *Journal of the American Statistical Association, 63,* 1379-1389. https://doi.org/10.1080/01621459.1968.10480934

Sighomnou, D. (2004). *Analyse et redéfinition des régimes climatiques et hydrologiques du Cameroun: Perspective d'évolution des ressources en eau*. Thèse de Doctorat d'État, Faculté de Sciences, Université de Yaounde I.

Svoboda, M., Hayes, M., & Wood, D. (2012). *Standardized Precipitation Index User Guide*. World Meteorological Organization: Geneva, Switzerland.

Tabari, H. (2020). Climate Change Impact on Flood and Extreme Precipitation Increases with Water Availability. *Scientific Reports, 10,* Article No. 13768. https://doi.org/10.1038/s41598-020-70816-2

Tanessong, R. S., Vondou, D. A., Djomou, Z. Y., & Moudi, P. I. (2017). WRF High Resolution Simulation of an Extreme Rainfall Event over Douala (Cameroon): A Case Study. *Modeling Earth Systems and Environment, 3,* 927-942. https://doi.org/10.1007/s40808-017-0343-7

Tchekote, H., Djofang, N. P., Ndongo, B., & Atekoa, M. F. B. (2019). Enjeux socio-économique et environnementaux de l'occupation des zones à risques d'inondation du bassin versant de l'Abiergué (Yaounde-Cameroun). *Revue Scientifique et Technique Foret et Environnement du Bassin du Congo, 13,* 69-80.

Tramblay, Y., Villarini, G., El Khalki, M. E., Gründemann, G., & Hughes, D. (2021). Evaluation of the Drivers Responsible for Flooding in Africa. *Water Resources Research, 57,* 2021WR029595. https://doi.org/10.1029/2021WR029595

WMO (2022). *State of the Global Climate 2021.* The World Meteorological Organization (WMO) Report WMO-No. 1290, Geneva.

Zogning, M. M. O. (2017). *Contribution des systèmes d'information géographique pour la cartographie des zones à risques d'inondation à Yaounde: Application au bassin versant du Mfoundi*. Mémoire de Master Spécialisé, Faculté des Sciences, Université de Liège, Belgique.

Zogning, M. M. O., Tsafelac, M., & Iaţu, C. (2011). Floods Risks in the Mfoundi Upstream Drainage Basin in Yaounde: A Response to Climatic Modifications or to Human Impacts? *Present Environment and Sustainable Development, 5,* 33-44.

Zogning, M. M. O., Tsafelac, M., Ursu, A., & Iatu, C. (2016). Contribution of Geographic Information Systems for the Mapping of Flooding Factors in Yaounde: The Case Study of Mfoundi Upstream Watershed. *De Gruyter PESD, 10,* 217-234. https://doi.org/10.1515/pesd-2016-0019